NASA TECHNICAL NOTE

NASA TN D-4814

THE DESIGN OF A PULSE POSITION MODULATED (PPM) OPTICAL COMMUNICATION SYSTEM

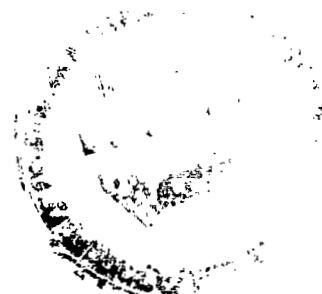*by*

Sherman Karp

Electronics Research Center
Cambridge, Mass.

and

Robert M. Gagliardi

University of Southern California
Los Angeles, Calif.

THE DESIGN OF A PULSE POSITION MODULATED (PPM)

OPTICAL COMMUNICATION SYSTEM

By Sherman Karp

Electronics Research Center
Cambridge, Mass.

and

Robert M. Gagliardi

University of Southern California
Los Angeles, Calif.

NATIONAL AERONAUTICS AND SPACE ADMINISTRATION

THE DESIGN OF A PULSE POSITION MODULATED (PPM) OPTICAL COMMUNICATION SYSTEM

By Sherman Karp
Electronics Research Center
and
Robert M. Gagliardi
University of Southern California

SUMMARY

In recent literature the advantages of an idealized narrow width pulse position modulated (PPM) optical communication system, using coherent sources and direct photo-detection, have been shown. In this report, the practical design of such an operating PPM link is considered. System performance, in terms of error probabilities and information rates, are derived in terms of key parameters, such as power levels, number of PPM signals, pulse width, and bandwidths. Both background radiation and receiver thermal noise are included. Design procedures utilizing these data are outlined. Whenever possible, optimal design values and parameter trade-offs, in terms of maximizing information rate or minimizing transmitter power, are shown. The effect on performance of photomultipliers and their inherent statistics is also presented. Although the basic analysis is derived in terms of photon "counts," the necessary system optics equations are introduced to allow for overall optical hardware design. The primary underlying assumption is that synchronization is maintained at all times between transmitter and receiver.

INTRODUCTION

With the development of coherent sources in the optical region of the spectrum, there has been an increasing interest in the design of optical communication systems (refs. 1-6). The direct detection of optical radiation is presently restricted to photo-detection surfaces for which it has been shown that the released electrons obey Poisson statistics (refs. 7,8). In this case investigators have shown the advantages of using narrow width pulse position modulation (PPM) as the principal mode of communication (ref. 3); that is, coding information into one of M possible signals and transmitting it as a pulse of optical energy placed in one of M adjacent time intervals. It had been shown (refs. 1-3) that idealized versions of such systems optimize performance in terms of various "distance" criteria, and in terms of overall error probability, for cases of most interest. Therefore, procedures for the practical design of an

M-ary low "duty cycle" PPM optical communication system will be presented in this report. In particular, performance characteristics in terms of key system parameters will be derived, with emphasis on hardware limitations and interference effects.

Consider the PPM optical communication system shown in Figure 1. The transmitter is a monochromatic optical source operating at a fixed frequency. Information is sent by transmitting one of M signals as a pulse of optical energy at the same frequency, located in one of M adjacent time intervals, each ΔT seconds wide. It is assumed that complete synchronization between transmitter and receiver is maintained at all times; i.e., time coherent operation. The optical receiver detects the transmitted signal by attempting to determine the optical energy in each possible time slot, selecting the signal corresponding to the maximal energy. In direct photodetection this is equivalent to "counting" the number of released electrons in each ΔT interval. Background radiation entering the photodetector acts as erroneous energy, causing signalling errors.

ONE OF
M SIGNALS

| OPTICAL SOURCE | PHOTO DETECTOR | + ⊕ + | CURRENT INTEGRATOR $\frac{1}{\Delta T} \int_0^{\Delta T}$ | MAX. LIKELIHOOD DECISION |

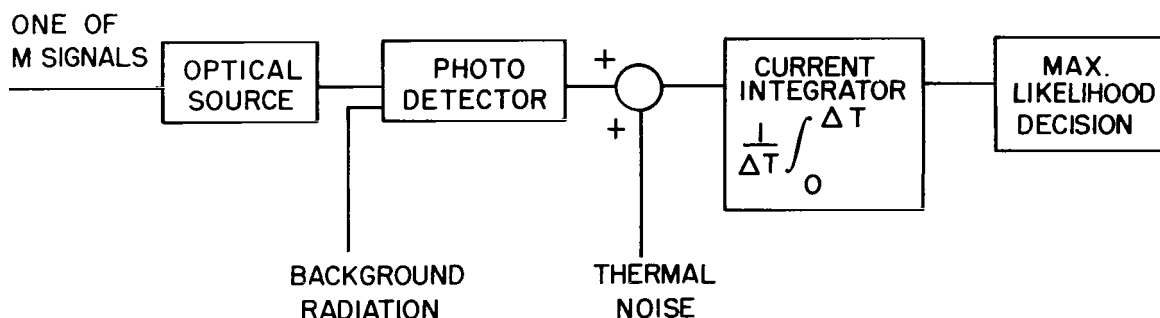BACKGROUND RADIATION   THERMAL NOISE

Figure 1.- Maximum likelihood processor

In practical systems, photomultipliers are often used to afford an improvement in photodetection (i.e., a gain in numbers of released electrons), but, unfortunately, they often behave randomly, which complicates system design. In addition, additive thermal noise may occur after photodetection. This tends to cause further errors in signal-decisioning. Both these latter effects will be considered subsequently.

As optical radiation impinges upon a photodetecting surface, a series of electrons are released, each producing a current pulse $eh(t-t_m)$ where e is the electron charge, t_m is the time of release, and $h(t)$ represents the current motion. The function $h(t)$ is pulse-like, having a time width roughly equal to the

2

inverse of the photodetector bandwidth. The function h(t) is assumed to be identical for all electrons, and the area of h(t) is assumed to be normalized to unity. In the absence of thermal noise, the output voltage across a resistor R of the normalized current integrator, when sampled after ΔT seconds of integration, is then

$$V = \frac{Ke}{\Delta T} R \qquad (1)$$

where K is the number of electrons released during the ΔT second integration period. This result neglects "end effects," that is, assumes h(t) can be considered an "impulse" function with respect to the integrating time ΔT. Thus, the integrator sample is proportional to the number of electrons released in the preceding ΔT time interval, and therefore "counts" electrons. The average number of electrons produced in the time interval ΔT as a result of the received radiation from the transmitter will be denoted K_S, and is proportional to the received transmitter energy, that is

$$K_S = \frac{\eta P_R \Delta T}{hf} \qquad (2)$$

where η is the photodetector efficiency, P_R is the received peak optical signal power in watts, f is the mode (transmitter) frequency and $h = 6.6 \times 10^{-34}$ joules-sec. The received power can be related to the system optics by

$$P_R = \left(\frac{d}{\theta r}\right)^2 P_T L \times 10^{-4} \qquad (3)$$

where d is the optical diameter in cm, r is the range in meters, θ is the divergence of the antenna in radians, P_T is the peak transmitter power, and L is the transmitting optics loss. The peak transmitter power can be converted to average transmitter power by dividing it by M, the number of signalling intervals.

Similarly, the average number of electrons in a time interval ΔT produced by the background radiation received by the optical collector may be denoted by K_N. Thus,

$$K_N = \frac{\eta P_N \Delta T}{hf} \qquad (4)$$

where now P_N is the received background radiation average power. This is generally written as

$$P_N = N_\lambda A_R L_O \Omega \; \Delta\lambda \qquad\qquad (5)$$

where N_λ is the background spectral radiance (watts/area-solid angle-bandwidth), L_O is the optical loss, A_R is the area of the collector, Ω is the resolution of the receiver (solid angle), and $\Delta\lambda$ is the optical bandwidth.

Note that with P_N held constant, the average number of "noise" electrons K_N is proportional to ΔT. This clearly indicates the advantage gained by low "duty cycle" operation, i.e., using signal intervals as narrow as possible, which decreases the amount of interfering radiation. The minimum value for ΔT, however, is approximately $1/\Delta\lambda$, for then the assumption of fixed noise power P_N is no longer valid. (For optical filters on the order of 5 Å, ΔT widths of 10^{-11} to 10^{-12} second are feasible.)

The number of electrons counted in a signalling interval (i.e., an interval ΔT containing transmitter energy) is then a Poisson random variable, the average value of which is $K_S + K_N$. For non-signalling intervals the average value is K_N. Note the system has been tacitly assumed to be synchronized; that is, the integration occurs exactly during the ΔT data intervals. The maximum likelihood of processing corresponds to counting the number of electrons in each of the M intervals and selecting the interval with the largest count as the proper PPM signal. Allowing for likelihood draws (in which case a random selection is made among the drawees), the probability of making a correct decision is

$$P_D = \sum_{r=0}^{M-1} \frac{1}{r+1} \begin{bmatrix} \text{Probability that the correct} \\ \text{interval count equals r other} \\ \text{interval counts and exceeds} \\ \text{the remaining M - r+1} \end{bmatrix}.$$

Temporarily neglecting the additive thermal noise and taking into account all the ways in which the correct interval count can equal r other interval counts yields:

4

$$P_D = \sum_{x=1}^{\infty} \sum_{r=0}^{M-1} \frac{1}{r+1} \binom{M-1}{r} \frac{\left(K_S + K_N\right)^x}{x!} e^{-\left(K_S + K_N\right)}$$

$$\left[\sum_{i=0}^{x-1} \frac{K_N^{\,i}}{i!} e^{-K_N}\right]^{M-1-r} \left[\frac{K_N^{\,x}}{x!} e^{-K_N}\right]^{r} + \frac{1}{M} e^{-\left(K_S + MK_N\right)} \tag{6}$$

Using the identity:

$$\sum_{r=0}^{M-1} \frac{(m-1)!}{(r+1)!\,(M-1-r)!} A^{M-1-r} B^r = \frac{A^{M-1}}{M\left(\frac{B}{A}\right)} \left[\left(1 + \frac{B}{A}\right)^M - 1\right]$$

one can rewrite Eq. (6) as

$$P_D = \sum_{x=1}^{\infty} \left\{ \frac{\left(K_S + K_N\right)^x}{x!} e^{-\left(K_S + K_N\right)} \left[\sum_{i=0}^{x-1} \frac{K_N^{\,i}}{i!} e^{-K_N}\right]^{M-1} \right.$$

$$\left. \left[\frac{(1 + a)^M - 1}{Ma}\right] \right\} + \frac{1}{M} e^{-\left(K_S + MK_N\right)} \tag{7}$$

where

$$a = \frac{K_N^{\,x}}{x! \sum_{i=0}^{x-1} \frac{K_N^{\,i}}{i!}} \quad .$$

The above result is amenable to computation and can be used in
system design to obtain performance characteristics for M-ary
operation with fixed parameter values. An exemplary plot is
shown in Figure 2 in which error probability $P_E = 1 - P_D$ is
plotted versus M for fixed values of K_S and K_N. The results
show the degradation in system performance as M is increased.

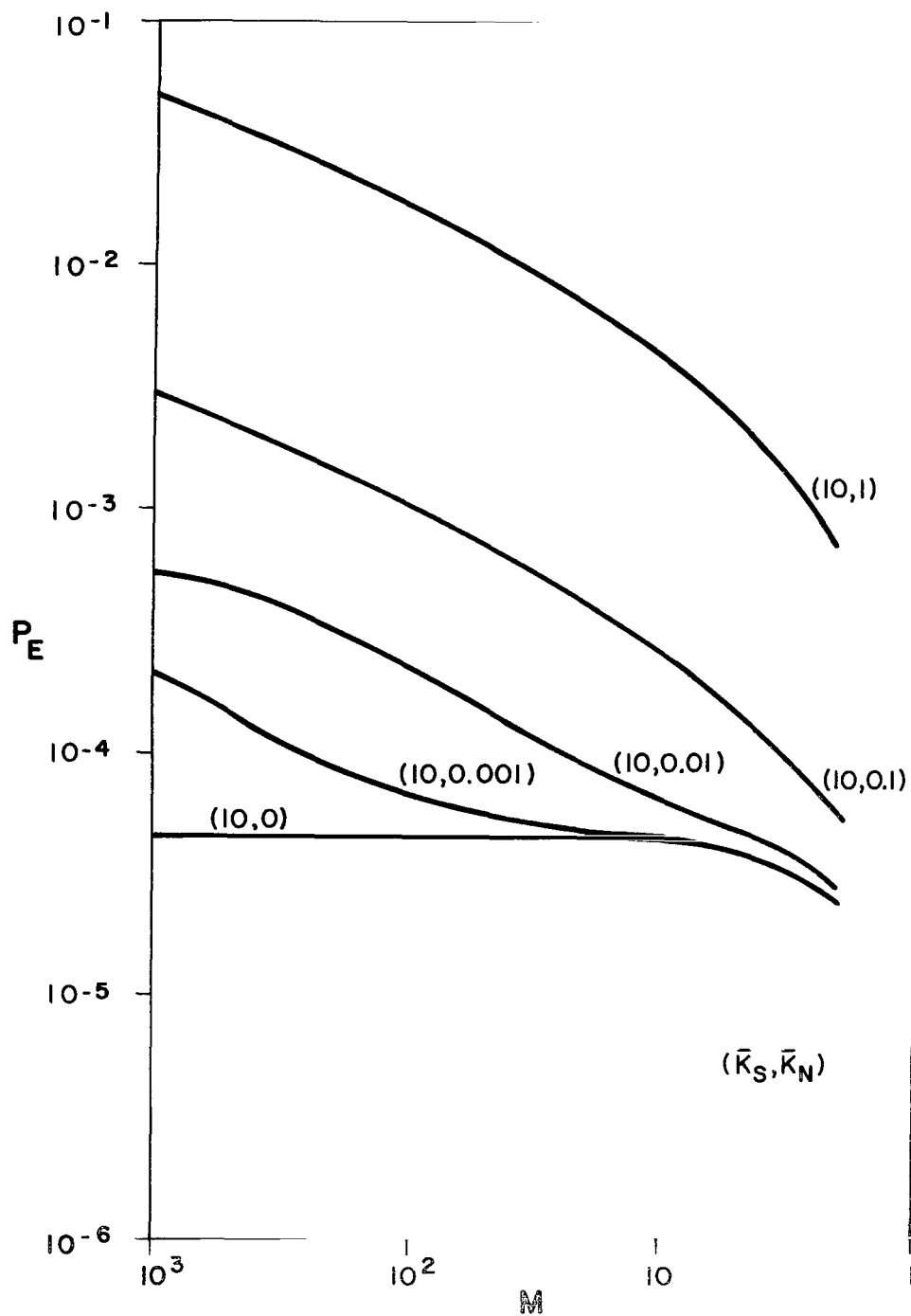Figure 2.- Error probability versus M

This can be attributed to the increase in likelihood draws as the number of intervals increases. Note that P_E depends upon both K_S and K_N, and not simply upon their ratio, so that a complete catalog of P_E curves is required to handle all design conditions (ref. 9).

Previously it was stated that the signal intervals ΔT should be as narrow as the optical bandwidths allow. This fact can be shown quantitatively by examining P_E as a function of ΔT, when P_N is assumed to be fixed. This is shown, for example, in Figure 3, where M = 2 and P_N is constrained such that the average electron noise count in an interval T_o is 10. The probability of error is plotted versus $\Delta T/T_o$, the "duty cycle" of the transmitter. Since K_S is held fixed throughout each curve, the transmitter peak power must necessarily increase proportionally, as is obvious from Eq. (2). Note that the error probability decreases monotonically as ΔT decreases. The minimum values at $\Delta T = 0$ are shown, but operation at these values implies infinite optical bandwidth. This minimum value is precisely the probability that a pro count occurs in signalling interval (which is also the noise count of the non-signalling intervals) and the receiver randomly selects incorrectly. It is also interesting to note that the pulse width ΔT is not particularly significant at low values of K_S. As K_S increases, however, the duty cycle begins to play a paramount role in the resulting error probability. Thus, attempts to increase bandwidth will have a direct payoff in system operation.

It is generally tempting for communication engineers to base system design in terms of signal-to-noise ratios. Typically, this is defined as the ratio of the squared average signal electron count to the variance of the count with background noise (ref. 5). In terms of a previous notation this becomes:

$$\left[\frac{S}{N}\right] = \frac{K_S^2}{K_S + K_N} \quad . \tag{8}$$

To indicate the difficulty in basing design purely upon the signal-to-noise ratio, consider the following comparison: Let $K_S = 10$ and $K_N = 10$; then $[S/N] = 5$ and, from Figure 2, $P_E = 3 \times 10^{-2}$. On the other hand, consider the case when $K_S = 5$ and $K_N = 0$. Again $[S/N] = 5$, but now $P_E = 3 \times 10^{-3}$. Thus, with less signal energy, detection has been improved an order of magnitude with the same signal-to-noise ratio. This is due to the fact that P_E in Eq. (7) depends upon signal energy K_S and noise energy K_N and not only upon the ratio. It is precisely
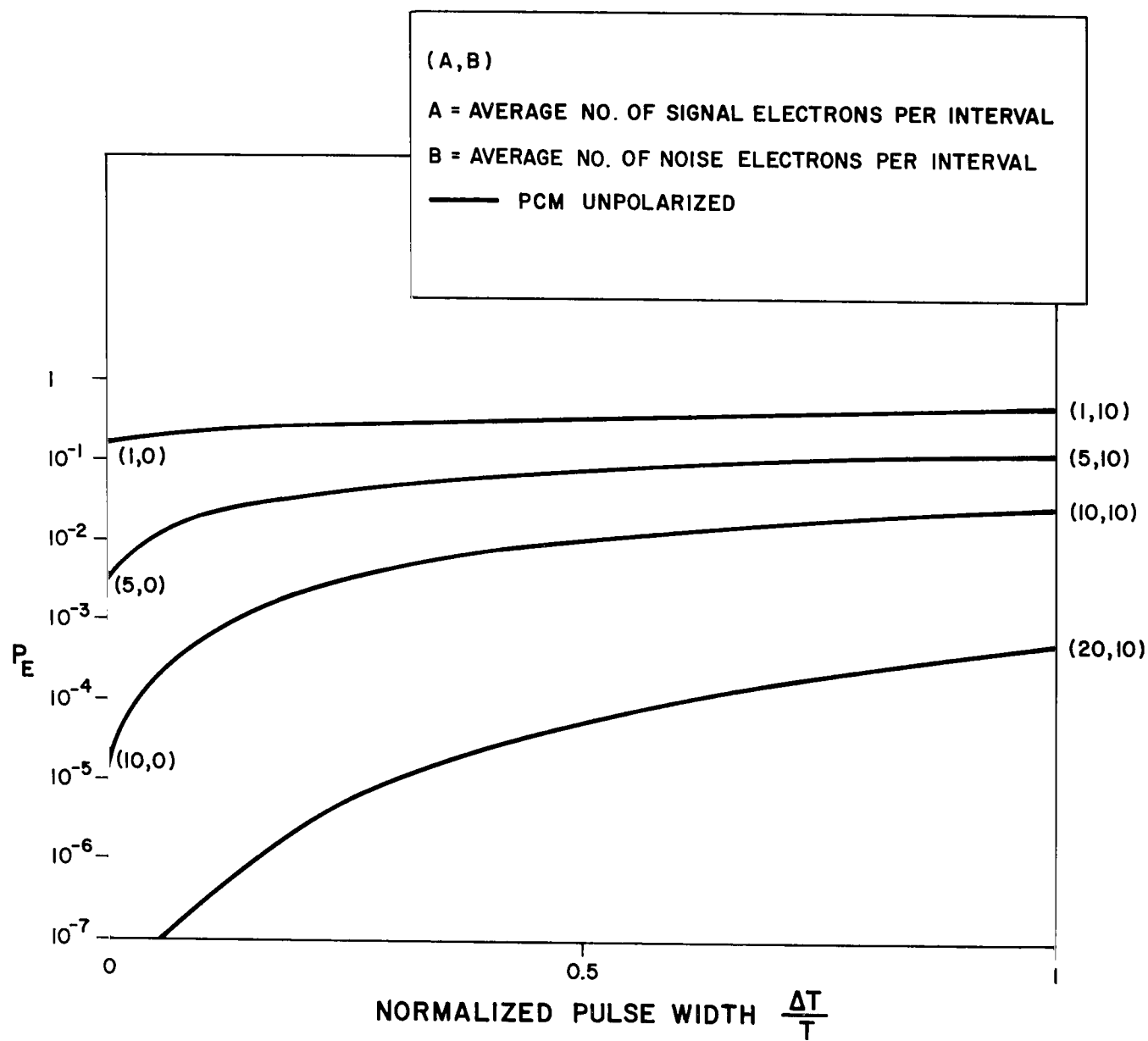
7

Figure 3.- Error probability versus normalized pulse width

this point that distinguishes the Poisson detection problem from the analogous problem of transmitting one of M orthogonal signals over a Gaussian additive channel of equal noise power.

It is also of interest to determine how the signal-to-noise ratio and error probability are related in general. By solving for K_S in Eq. (8) one obtains:

$$K_S = \frac{1}{2} \frac{S}{N} \left[1 + \sqrt{1 + \frac{4K_N}{S/N}} \right] \qquad (9)$$

which can be inserted into Eq. (7). One can then plot P_E versus K_N, for fixed values of S/N and M, as shown in Figure 4. For large values of K_N, P_E approaches Erf (S/2N), which is identical to the error probability of orthogonal coherent signalling in Gaussian noise with a signal-to-noise ratio of S/N. Since this approach is asymptotic from below, the Gaussian case will always be inferior to the Poisson case for the same signal-to-noise ratio. This point is also in agreement with results showing the equivalence of optimum Poisson processing and optimum Gaussian processing for large values of background noise power (refs. 1,4). Notice again that, to maintain the same signal-to-noise ratio, K_S must be increased. Lastly, it can be seen that even if noise background is negligible, $K_N \to 0$, the signalling error probability does not go to zero, but rather approaches

$$P_E \Big|_{K_N \to 0} = \frac{1}{2} e^{-K_S} . \qquad (10)$$

This is the same as the minimum values (at $\Delta T = 0$) shown in Figure 3.

EFFECT OF THERMAL NOISE AND PHOTOMULTIPLIERS

So far in the analysis, the effect of additive thermal noise, which adds a random variable to the integrator output sample of Eq. (1), has been neglected. This complicates the original assertion that the receiver counts exactly the number of electrons at the photodetector output. Since this is the crux of the maximum likelihood direct detection system, it would be worthwhile to investigate this problem in more detail. Suppose, for example, one considers the current resulting from the flow of a signal photo-electron during a time interval $\Delta T = 10^{-9}$ second. The sample value at the integrator output across a

$$p\left(\frac{S}{N}\right) = \frac{1}{2} e^{-\frac{S}{N}}$$

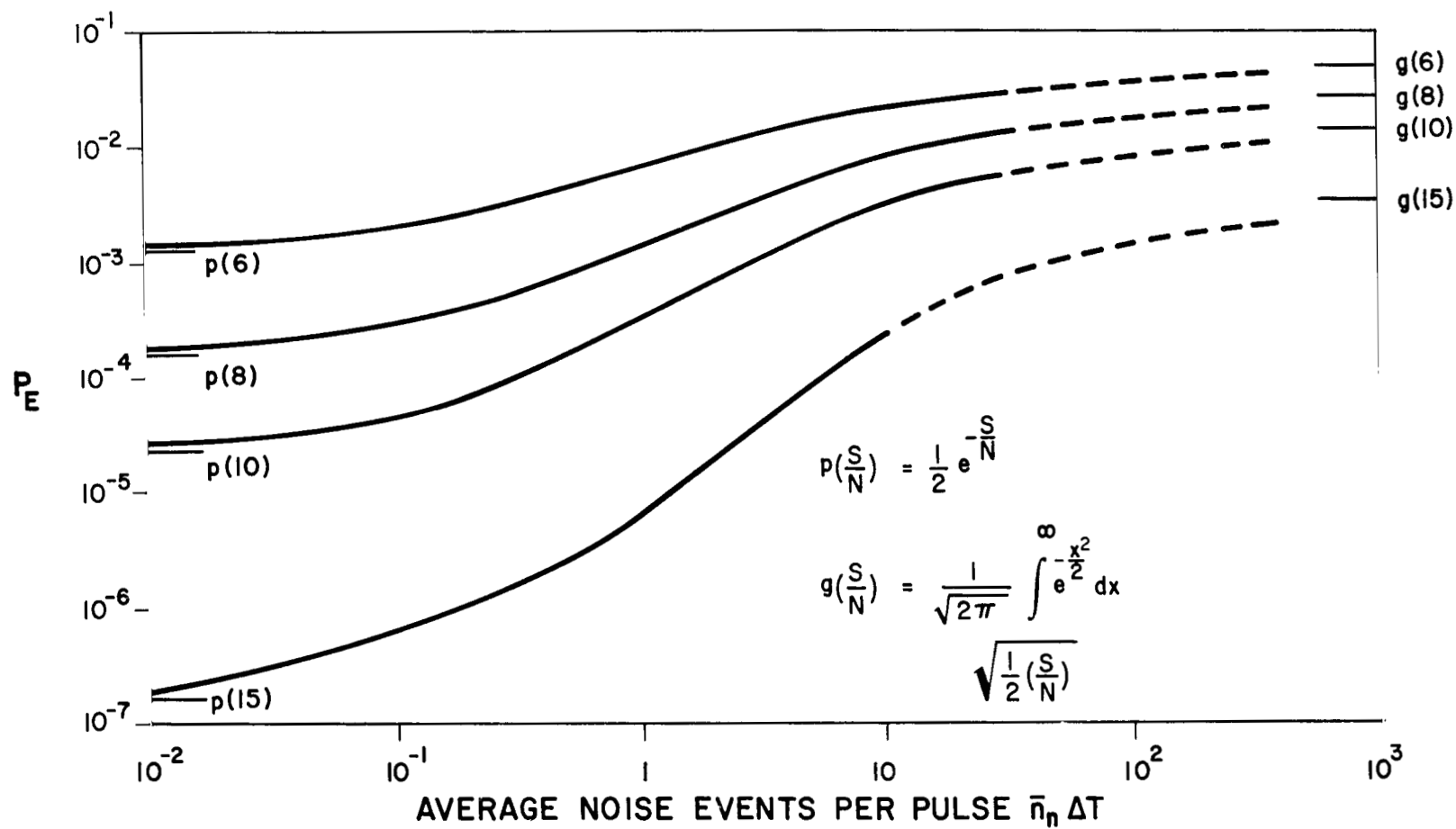$$g\left(\frac{S}{N}\right) = \frac{1}{\sqrt{2\pi}} \int_{\sqrt{\frac{1}{2}\left(\frac{S}{N}\right)}}^{\infty} e^{-\frac{x^2}{2}} dx$$

Figure 4.- Probability of error for fixed signal-to-noise ratio versus noise background

50-ohm resistor from this electron would be 8×10^{-9} volt. Now if the receiver operated at room temperature, the thermal additive noise would contribute an integrator noise voltage, the root mean square value of which is approximately 28×10^{-6} volt ($R = 50$ ohms, temp = $300^\circ K$). Clearly, the count of a single electron could not easily be made in such a poor signal and noise condition. Photomultipliers exist, however, which effectively amplify the current effect of each photo-electron, resulting in a larger photo-electron "count" at the integrator output. Let this amplification factor be A, so that each photo-electron contributes a current value $Ae/\Delta T$ at time of sample. It would be interesting to determine the effect of A on P_D in Eq. (7) when Gaussian white thermal noise of one-sided spectral level N_O is added at the integrator input. If one assumes each electron receives the same photomultiplier gain A, the sample value due to the photodetector output is

$$ V = \frac{KeA}{\Delta T} R \tag{11} $$

where K is again the number of electrons produced during the interval ΔT. With Poisson statistics for the electron count during the ΔT interval, the probability density of V is then

$$ P_V(V) = \sum_{j=0}^{\infty} \left[\frac{\overline{K}^j}{j!} e^{-\overline{K}} \right] \delta(V - jeA\beta R) \tag{12} $$

where $\delta(x)$ is the Dirac delta function, $\beta = 1/\Delta T$, and $\overline{K}$ is the average value of K. The thermal noise is integrated by the integrator and adds to the integrator sample V a random variable that is Gaussian-distributed with zero mean and variance $N_O\beta$. Thus, the total integrator sample value z after ΔT seconds of "counting" has a probability density obtained by convolving the Gaussian density with the discrete density in Eq. (12), yielding:

$$ P_z(z,\overline{K}) = \sum_{j=0}^{\infty} \left[\frac{\overline{K}^j}{j!} e^{-\overline{K}} \right] G(z, jAe\beta R, N_O\beta) \tag{13} $$

where $G(a,b,c)$ denotes a Gaussian density in the variable a with a mean b and a variance c. Observe that the sample probability densities are now continuous densities, and the probability of equal sample values occuring is zero; that is, there is a zero

probability of likelihood draws. Now the average count $\bar{K}$ is $K_S + K_N$ when a signal is present in the ΔT interval, and is K_N when the signal is absent. Therefore, the probability of a correct decision is simply the probability that the observable z after the correct interval exceeds the observable z after the M-1 remaining intervals. Hence:

$$P_D = \int_{-\infty}^{\infty} dz \; P_z(z, K_S + K_N) \left[\int_{-\infty}^{z} P_z(y, K_N) \; dy \right]^{M-1} . \quad (14)$$

This can be written more compactly as

$$P_D = \sum_{j=0}^{\infty} \frac{(K_S + K_N)^j}{j!} \; e^{-(K_S + K_N)} \int_{-\infty}^{\infty} dz \; G(z, \mu, \sigma^2) \psi^{M-1}(z) \quad (15)$$

where

$$\psi(z) = \frac{1}{2} \left\{ 1 + \sum_{j=0}^{\infty} \left[\frac{K_N^{\; j}}{j!} \; e^{-K_N} \right] \text{Erf} \left(\frac{z - j\mu}{\sqrt{2}\sigma} \right) \right\}$$

$$\mu = Ae\beta R$$

$$\sigma^2 = N_o \beta$$

and Erf (x) is the error integral. Equation (15) has been evaluated for several values of K_S and K_N and is shown in Figure 5, with $\beta = 10^9$ Hz and N_o corresponding to a noise temperature of 300°K with a 50-ohm load. The asymptotic values for large photomultiplier gains are precisely the values obtained by Eq. (7). At low gains, however, the thermal noise becomes the dominating source of error, and the probability of error increases rapidly. Note that to overcome the thermal environment a photomultiplier gain of about 10^4 is necessary for all the operating conditions shown. For other thermal environments one can use, as a rule of thumb,

$$A > 600 \sqrt{\text{temp}}$$

obtained by directly scaling the foregoing results.

12

Figure 5.- Probability of error for ideal photomultiplier
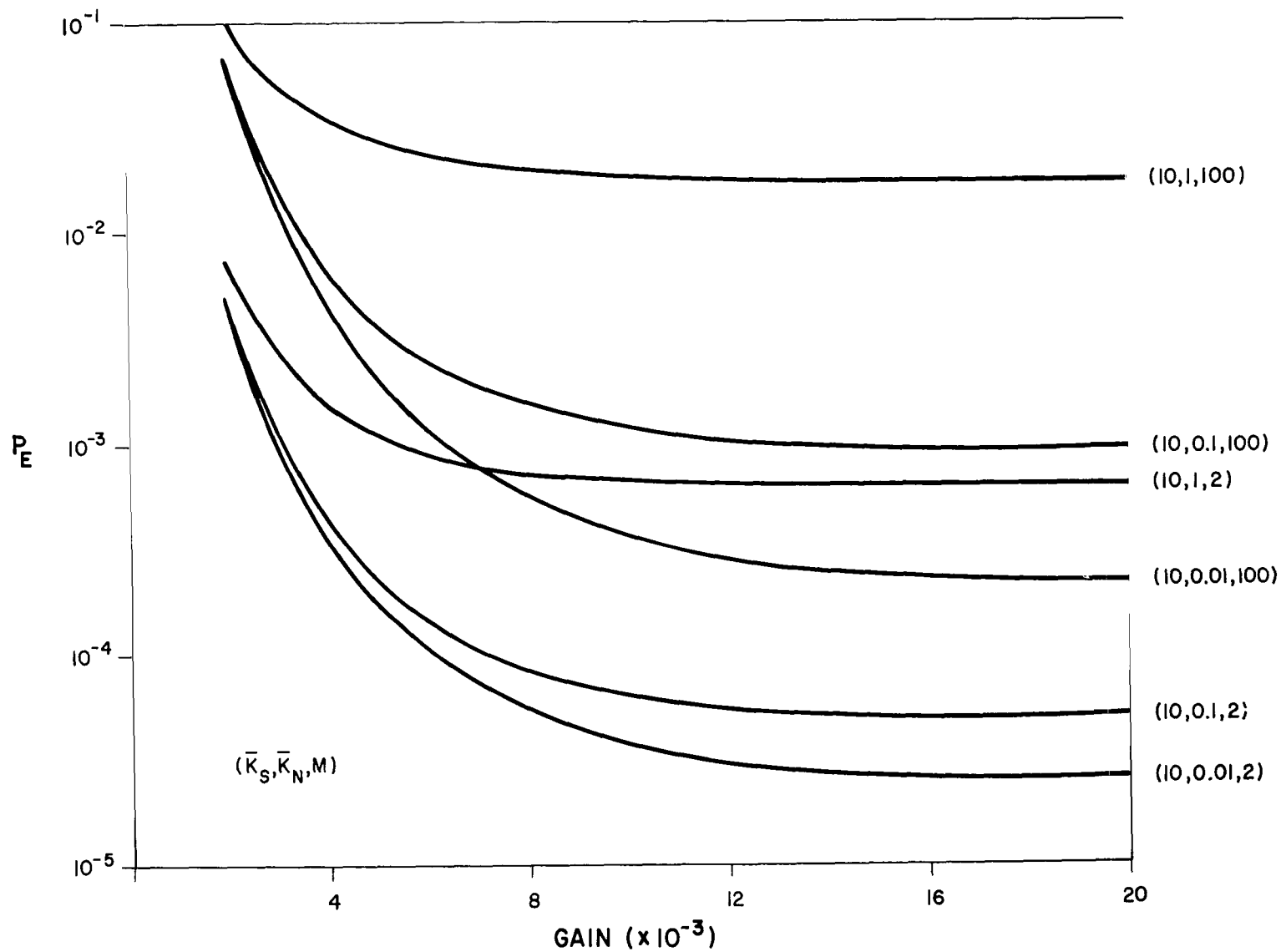
In the previous analysis we have assumed that the multiplier gain was a constant; that is, was the same for all photoelectrons. In practice, however, the gain itself is generally a random variable (ref. 10) with a variance, or "spread," usually taken as a percentage of the mean gain. It would be desirable now to recompute P_D under this situation. If one lets A_i be the electron gain of the ith released photo-electron, the integrator sample value for K electrons is then

$$V = \sum_{i=1}^{K} A_i e\beta R \tag{16}$$

where each A_i is an independent random variable with probability density $P_A(x)$. The probability density of V is then obtained from

$$P(V) = \sum_{K=0}^{\infty} P(V/K) P(K) \tag{17}$$

where $P(V/K)$ is the conditional density of V, given K photo-electrons. Hence, from Eq. (16):

$$P(V/K) = \left(\frac{1}{e\beta R}\right)^K \left[P_A\left(\frac{V}{e\beta R}\right) \underset{K-1}{\otimes} P_A\left(\frac{V}{e\beta R}\right)\right] \tag{18}$$

where $\underset{K}{\otimes}$ denotes K-fold convolution.

Assume $P_A(x)$ is Gaussian with mean A and standard deviation $\alpha A/2$, where $0 \leq \alpha \leq 1$ represents a percentage of the gain. Then Eq. (18) is the Gaussian random variable with mean $KAe\beta$ and variance $K([\alpha A/2]e\beta R)^2$ so that Eq. (17) becomes:

$$P(V) = \sum_{i=0}^{\infty} \frac{\overline{K}^i}{i!} e^{-\overline{K}} G\left(V, iAe\beta R, i([\alpha A/2]e\beta R)^2\right) \tag{19}$$

14

If one adds the sample contribution due to the thermal noise, the sample z has a probability density

$$P_z(z,\overline{K}) = \sum_{i=0}^{\infty} \frac{\overline{K}^i}{i!} e^{-\overline{K}} G\left(V, iAe\beta R, i([\alpha A/2]e\beta R)^2 + N_o\beta\right). \quad (20)$$

Note the above equation is identical to Eq. (13), except for the variance terms in the Gaussian densities, and specializes to Eq. (13) for $\alpha = 0$. Hence, the probability of detection is given exactly by Eq. (14), with the variance σ^2 replaced by the above variance. The resulting error probabilities are shown in Figure 6 as a function of the "spreading" parameter α, using parameters as in Figure 5. Although the results vary somewhat as a function of signal and noise, one observes that for mean gains between 10^4 and 10^5 the error probabilities obtained earlier (Figure 2) are valid with gain spreads as high as 30 to 40 percent. Even with spreads as high as 70 percent, the results indicate only about a factor of 2 increase in error probability. The primary conclusion then is that with suitably high mean photomultiplier gains, system error probabilities can basically be divorced of additive thermal noise effects. In this case the error curves plotted in Figure 2 represent the overall system error probabilities.

The previous results also imply that a device average gain-to-spread ratio should be as large as possible for best operation. Consider an idealized photomultiplier characterized as a Poisson branching process (ref. 10). Every photoelectron emitted from the photoemissive surface impinges on the first stage of the device and releases K secondary electrons which are Poisson distributed in number with parameter δ_1. The secondary electrons are then focused on the second stage where the same effect occurs. This process continues on through n stages resulting in a large electron flow at the anode for each photoelectron emitted. The distribution of electrons at the anode output is quite complicated but is unimodal and quite easily fitted with a gaussian distribution as we have already done. In our calculations of error probability the two important parameters emerging were the mean gain of the device, A, and the mean gain to r.m.s. gain ratio, Γ. For the idealized photomultiplier the two parameters can be calculated in a straightforward manner and are, in our previous notation,
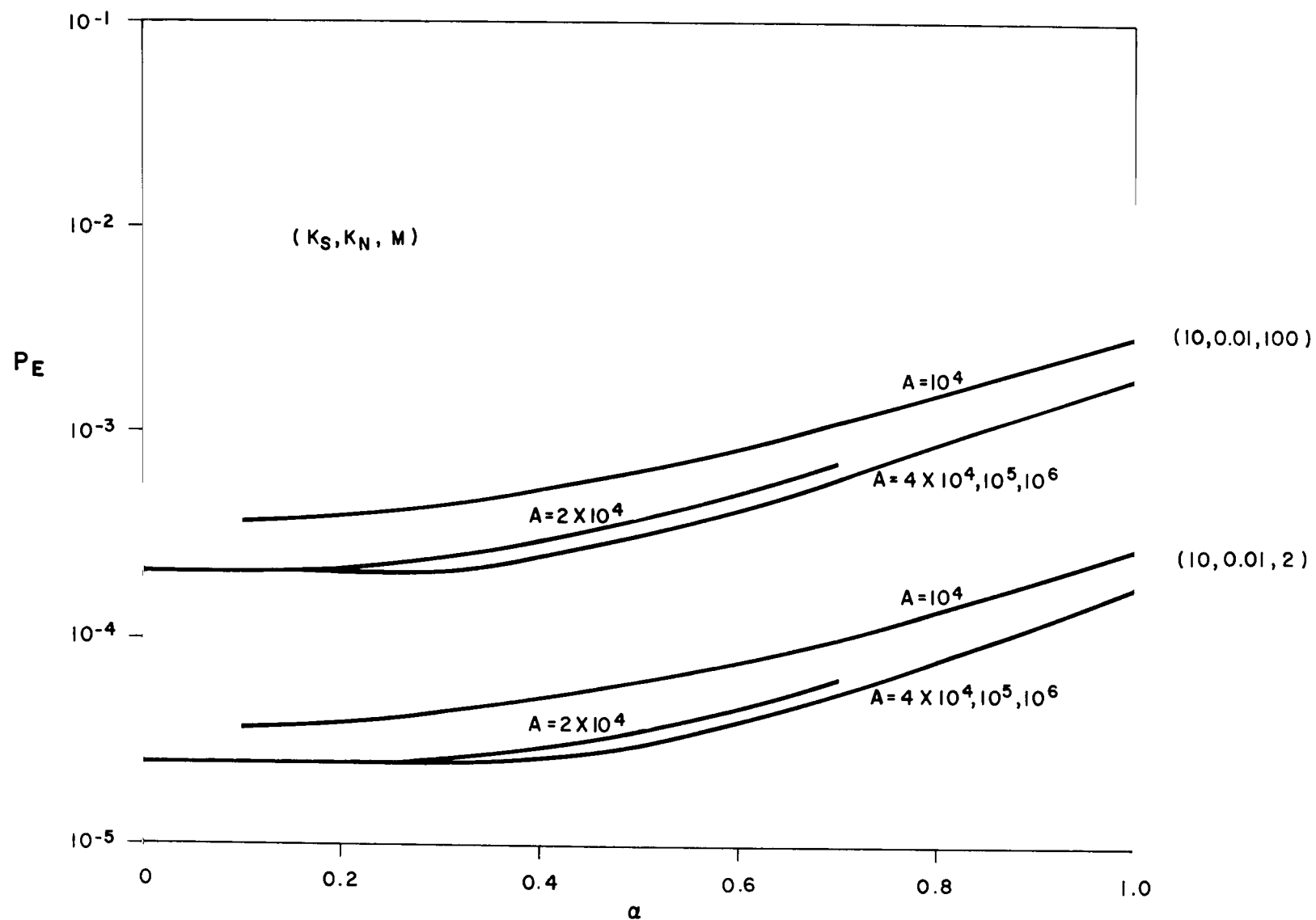
$$A = \prod_{i=1}^{n} \delta_i$$

15

Figure 6.- Probability of error for photomultiplier model

$$\Gamma = \frac{2}{\alpha} = \sqrt{\left[1 + \frac{1}{\delta_2} + \frac{1}{\delta_2 \delta_3} + \frac{1}{\delta_2 \delta_3 \delta_4} + \cdots\right]^{\delta_1}}$$

Notice that Γ is almost completely characterized by the first stage gain δ_1 (a minor contribution is also made by the second stage). Thus we can relate α directly to the gain of the first stage by

$$\alpha \cong \frac{2}{\sqrt{\delta_1}} \quad .$$

For "photon counting," Figure 6 indicates that $\alpha < .4$ or that

$$\frac{2}{\sqrt{\delta_1}} < .4 \Rightarrow \delta_1 > 25 \quad .$$

To take into account the effects of the remaining n-1 stages assume $\delta_2 = \delta_3 = \ldots = \delta_n = \delta$. Then

$$\sum_{i=0}^{n} \left(\frac{1}{\delta}\right)^i = \frac{1 - (1/\delta)^{n+1}}{1 - (1/\delta)} < \frac{1}{1 - (1/\delta)} = \frac{\delta}{\delta - 1} \quad .$$

Therefore δ_1 should be increased by $\delta/(\delta - 1)$. Typically $\delta = 4$ so that

$$\delta_1 > 25 \cdot \frac{4}{3} = 33 \quad .$$

INFORMATION RATE OF A PPM SYSTEM

So far, only one aspect of system performance has been analyzed, i.e., error probabilities. The actual information rate that the link achieves is another important design consideration. As stated, the transmitter sends optical energy in one of

M time intervals ΔT seconds wide, thereby transmitting one of M possible signals in $M\Delta T$ seconds or at a rate $\log_2 M/M\Delta T$ bits/sec. The receiver correctly determines the true signal with probability $1 - P_E$ and is in error with probability P_E. Because of symmetry the erroneous signal may be interpreted, equal-likely, as any of the M-1 incorrect signals. Thus, the overall channel may be depicted as an M-ary symmetric channel in which each of the M possible transmitter signals is converted to itself with probability $1 - P_E$, and is converted to each other signal with probability $P_E/M-1$. The information rate for such a channel is known to be

$$R = \frac{\log_2 M + P_E \log_2 \left(\frac{P_E}{M-1}\right) + \left(1-P_E\right) \log_2 \left(1-P_E\right)}{M\Delta T} \tag{21}$$

For convenience one may denote this as

$$R = \frac{C\left(K_S, K_N, M\right)}{M\Delta T} \tag{22}$$

to emphasize the dependence of the numerator on the stated parameters. By using Eq. (22) and the families of error probability curves as shown in Figure 2, the rate R can be evaluated by straightforward substitution. Although specific curves for such a computation are not shown here, it suffices to note that if K_S and K_N are such that $P_E < 10^{-1}$, Eq. (22) is to a good approximation,

$$R \approx \left(1-P_E\right) \frac{\log_2 M}{M\Delta T} = \frac{\log_2 M}{M\Delta T} - P_E \frac{\log_2 M}{M\Delta T} \tag{23}$$

If one interprets the rate R as the source rate minus the equivocation of the channel, the PPM optical system behaves approximately as if a source rate of $\log M/M\Delta T$ is passed into a channel of equivocation $P_E \log M/M\Delta T$. As noted in Eq. (10), even if $K_N \to 0$ (no background interference), $P_E \to \exp(-K_S)/2$ so that the equivocation is not due entirely to the background noise.

The use of Eq. (22) and the previous equations are helpful in determining the rate, given operating parameters. However,

the converse design problem, determining particular parameter values that achieve a desired rate, is not so straightforward. This is due to the fact that the rate is a somewhat complicated function of the parameters. Two aspects of this design problem that have practical application under certain operating conditions will be considered here:

(1) The word period $T = M\Delta T$ is held fixed while the information bandwidth $\beta = 1/\Delta T$ is allowed to vary and,

(2) System bandwidth β is held fixed while the word period is allowed to vary.

In both cases we are interested in the relationship between the rate R and the transmitter parameters K_S and M, assuming the noise power is held fixed.

Fixed Work Period

It is assumed here that ΔT is allowed to vary with M so as to maintain $T = M\Delta T$ constant. Thus, the system "squeezes" more signals into the T second period as M increases. The resulting rate is then

$$R = \frac{C\left(K_S, K_{NT}/M, M\right)}{T} \tag{24}$$

where K_{NT} is the noise energy in T. Thus, the rate depends only upon the numerator of Eq. (22). With K_S fixed, increasing M increases the source rate, but the error probability also increases, eventually reaching an asymptotic value of

$$P_E = \left[1 + K_S \frac{\left[K_{NT} - 1 + e^{-K_{NT}}\right]}{K_{NT}}\right] e^{-K_S}$$

for large M. The resulting system rate increases, to within a constant of the entropy of the alphabet, $\log_2 M/T$. Therefore, it is clear that if bandwidth is expendable, one will always increase the system rate for large M by increasing M. In a practical system, this implies that one should operate with as wide a bandwidth as possible to exploit fully the capability of

the PPM system. One would, therefore, naturally consider the design of a system for an arbitrary rate H, when the full bandwidth ($1/\Delta T$) of the system is limited.

Fixed Bandwidth

In this case ΔT is held constant (thereby fixing the noise energy in ΔT, K_N) so that both numerator and demoninator in Eq. (22) depend upon M, and the rate degrades quickly as M increases due to the log M/M dependence. A given rate, say H_O, may be obtained by many different combinations of K_S and M. Analytically, these equivalent operating points may be obtained graphically by noting that they are the values for which the numerator $C(K_S,K_N,M)$, considered as a function of M, intersect the straight line $H_O \Delta TM$. By plotting these functions, for various K_S, their intersection will identify (K_S,M) pairs which achieve the rate H_O. One may then decide on a particular operating point by invoking suitable design criteria. For example, one may select the smallest M from among the candidate pairs, which then minimizes the word period $T = M\Delta T$. Alternatively one may choose to minimize the average transmitter power per information bit, which is proportional to K_S/C. In the latter case, therefore, one would select the operating pair (K_S,M) for which K_S/C is minimal. An application of this procedure is given in the next section.

AN EXAMPLE--REAL TIME TELEVISION FROM DEEP SPACE

To illustrate the design procedures outlined in this report, a television system which will transmit in real time from deep space will be considered. System parameter values will be chosen to allow use of the previously derived data. These do not always reflect the optimum values or current state of the art. The following transmission parameters will be assumed.

Blue sky background

Distance -- 4×10^8 km

Optical loss -- 50%

Receiver diameter -- 16 meters (non-diffraction-limited)

Receiver temp -- 300^OK

Optical bandwidth -- 5Å

Quantum efficiency -- 20%

Resolution -- 1 arc sec

Photomultiplier gain -- $>10^5$

Optical frequency -- 5000 $\overset{\circ}{A}$

Signal bandwidth -- 10^9 Hz.

For real time television a rate of approximately 7×10^7 bit/sec
is required (corresponding to better than two samples per infor-
mation Hz and seven bits per sample coding). The objective here
is to determine design parameters for a PPM system that uses
minimal average transmitter power and a bit error probability no
greater than 10^{-4}. Using parameters of the above table in Eqs.
(4) and (5) yields $K_N = 0.01$ as the noise background count.
Following the discussion in the previous section, one may plot
$C(K_S,.01,M)$ as a function of M and determine the intersection
with the line $(H_0 \Delta T)M = (7 \times 10^{-2})M$, yielding the tabulation in
Table I.

TABLE I

K_S	M	K_S/C	K_S	M	K_S/C
.8	19	0.593	1.6	47	0.488
.9	23	0.552	1.8	52	0.496
1.0	28	0.506	2.0	55	0.508
1.2	35	0.494	5.0	95	0.792
1.4	42	0.484			

The minimal average transmitter power occurs when $K_S = 1.4$,
$M = 42$ which defines the PPM system. Using Eqs. (2) and (3) the
transmitter then requires 0.072 watt. The corresponding P_E can
be obtained from Eq. (7) to get the word error probability
(2.4×10^{-1}) for which the corresponding bit error probability
is approximately (ref. 9) $P_E/2 \simeq 10^{-1}$. Thus, the bit error is
larger than that derived and, in fact, will be further increased
by the thermal noise, as evidenced by the data of Figure 5.
(The figure shows a slight increase in P_E for $K_S = 10$ and $M = 2$
at photomultiplier gains of 10^4, and one can conclude the situa-
tion will be worse for $K_S = 1.4$ and $M = 42$). Thus, the minimal
power condition is not sufficient to obtain the desired P_E for
this example without coding.

To achieve the desired bit error probability Figure 2 shows that a system with $K_S = 10$ and $M = 100$ yields bit error probabilities $P_E/2 \approx 10^{-4}$ at the same noise level. One would expect no appreciable degradation from thermal noise, and Figure 6 indicates that only slight increases occur even with photomultipliers having "spreading" as high as 45 percent. The transmitter power, which no longer is minimal for the desired information rate, is found to be 0.25 watt, or an increase of 5.4 dB over the minimal average conditions.

CONCLUSION

In this paper, some design aspects of an optical M-ary pulse position modulated (PPM) communication system using photon counters (photodetectors followed by current integrators) at the receiver have been considered. The system considered transmits monochromatic optical energy in one of M time intervals, and the receiver determines the photon count (i.e., the received energy) in each interval and performs a maximum likelihood test to determine which signal is being received. Complete line synchronization is assumed to be maintained at all times. Performance characteristics are derived in terms of system parameters with both background radiation and thermal noise interference. In particular it is shown that, unlike the case of pure Gaussian additive noise, system performance does not depend on a few key parameters, but must be recomputed for different operating points. The important equations for deriving these characteristics are introduced. From these, design procedures are outlined which lead to best choices of transmitter power, numbers of signals, interval lengths, and so forth, in order to obtain desired error probabilities and information rates. In particular, the requirements imposed upon the individual components have been indicated and the strong and weak points in the overall system have been delineated. No attempt has been made to estimate the cost or weight in building such a system. This, in fact, would be premature since the technology required is in its infancy and undergoing swift and quite radical change. In addition, no discussion of methods to maintain link synchronization has been included, nor has any consideration of atmospheric effects other than a loss factor been made.

REFERENCES

1. Reiffen B., and Sherman, H.: An Optimum Demodulator for Poisson Processes. IEEE Proc., vol. 51, no. 10, pp. 1316-1320, October 1963.
2. Abend, K.: Optimum Photon Detection. IEEE Trans. on Information Theory, vol. 12, no. 1, pp. 64-65, January 1966.
3. Gagliardi, R.M., and Karp, S.: M-ary Poisson Detection and Optical Communications. NASA Technical Note TND-4623, Electronics Research Center, June 1968.
4. Helstrom, C.W.: Quantum Limitations on the Detection of Coherent and Incoherent Signals. IEEE Trans. on Information Theory, vol. IT-11, no. 4, pp. 489-491, October 1965.
5. Pratt, W.K.: Binary Detection in an Optical Polarization Modulation Communication Channel. IEEE Trans. on Communication Technology, vol. Com-14, no. 5, pp. 664-665, October 1966.
6. Karp, S.: A Statistical Model for Radiation with Applications to Optical Communications. PhD Dissertation, University of Southern California, January 1967.
7. Oliver, B.M.: Thermal and Quantum Noise. IEEE Proc., vol 53, pp. 436-454, May 1965.
8. Mandel, L.: Fluctuations of Light Beams -- Progress in Optics. E. Wolf, ed., J. Wiley, New York, 1963.
9. Karp. S., Hurwitz, M.G., and Gagliardi, R.M.: Error Probabilities for Maximum Likelihood Detection of M-ary Poisson Process in Poisson Noise, NASA Technical Note TND-4721, Washington, D.C., July 1968.
10. Gale, H.J., and Gibson, J.A.B.: Methods of Calculating the Pulse Height Distribution at the Output of a Scintillation Counter. J. Sci. Inst., vol. 43, pp. 224-228, 1966.
11. Viterbi, A.J.: Principles of Coherent Communication. McGraw-Hill, New York, 1966.

POSTMASTER: If Undeliverable (Section 158 Postal Manual) Do Not Return

"The aeronautical and space activities of the United States shall be conducted so as to contribute . . . to the expansion of human knowledge of phenomena in the atmosphere and space. The Administration shall provide for the widest practicable and appropriate dissemination of information concerning its activities and the results thereof."

— NATIONAL AERONAUTICS AND SPACE ACT OF 1958

NASA SCIENTIFIC AND TECHNICAL PUBLICATIONS

TECHNICAL REPORTS: Scientific and technical information considered important, complete, and a lasting contribution to existing knowledge.

TECHNICAL NOTES: Information less broad in scope but nevertheless of importance as a contribution to existing knowledge.

TECHNICAL MEMORANDUMS: Information receiving limited distribution because of preliminary data, security classification, or other reasons.

CONTRACTOR REPORTS: Scientific and technical information generated under a NASA contract or grant and considered an important contribution to existing knowledge.

TECHNICAL TRANSLATIONS: Information published in a foreign language considered to merit NASA distribution in English.

SPECIAL PUBLICATIONS: Information derived from or of value to NASA activities. Publications include conference proceedings, monographs, data compilations, handbooks, sourcebooks, and special bibliographies.

TECHNOLOGY UTILIZATION PUBLICATIONS: Information on technology used by NASA that may be of particular interest in commercial and other non-aerospace applications. Publications include Tech Briefs, Technology Utilization Reports and Notes, and Technology Surveys.

Details on the availability of these publications may be obtained from:

SCIENTIFIC AND TECHNICAL INFORMATION DIVISION

NATIONAL AERONAUTICS AND SPACE ADMINISTRATION

Washington, D.C. 20546